CHAPTER 2: The Nicotinic Pharmacophore: The Pyridine N of Nicotine and Carbonyl of ACh Hydrogen Bond Across a Subunit Interface to a Backbone NH*

2.1 ABSTRACT

Pharmacophore models for nicotinic agonists have been proposed for four decades. Central to these models is the presence of a cationic nitrogen and a hydrogen bond acceptor. It is now well-established that the cationic center makes an important cation-π interaction to a conserved tryptophan, but the donor to the proposed hydrogen bond acceptor has been more challenging to identify. A structure of nicotine bound to the acetylcholine binding protein (AChBP) predicted that the binding partner of the pharmacophore's second component was a water molecule, which also hydrogen bonds to the backbone of the complementary subunit of the receptors. Here we use unnatural amino acid mutagenesis coupled with agonist analogs to examine whether such a hydrogen bond is functionally significant in the α4β2 neuronal nAChR, the receptor most associated with nicotine addiction. We find evidence for the hydrogen bond with the agonists nicotine, acetylcholine, carbamylcholine, epibatidine, and cytisine, but do not find evidence for the hydrogen bond with varenicline. These data represent a completed nicotinic pharmacophore for most nicotinic agonists and offer insight into the design of new therapeutic agents that selectively target these receptors.

---

* *This chapter is adapted from:* Blum, A. P.; Lester, H. A.; Dougherty, D. A., Nicotinic pharmacophore: The pyridine N of nicotine and carbonyl of acetylcholine hydrogen bond across a subunit interface to a backbone NH. *Proceedings of the National Academy of Sciences of the USA* **2010,** *107*, (30), 13206-11. Copyright 2010 by the National Academy of Sciences. *The work described in this chapter concerning cytisine, varenicline and the A3B2 receptor was done in collaboration with Nyssa L. Puskar, Darren T. Nakamura, Ximena Da Silva Tavarres Bongoll, and Dr. Jai A. P. Shanata.*

2.2 INTRODUCTION

The nicotinic acetylcholine receptor (nAChR) is a pentameric, ligand-gated ion channel activated by the neurotransmitter acetylcholine (ACh), and also by nicotine and structurally related agonists.[1-3] Nicotinic receptors mediate fast synaptic transmission at the neuromuscular junction of the peripheral nervous system. In addition, a family of paralogous nAChRs termed the neuronal receptors function in the central nervous system and certain autonomic ganglia, and the addictive and cognitive properties of nicotine are associated with these neuronal receptors.[4, 5] Neuronal receptors comprised of α4 and β2 subunits are most strongly associated with nicotine addiction.[6-9] They are upregulated during chronic nicotine exposure and are implicated in various disorders, including Alzheimer's disease and schizophrenia, and in protection against Parkinson's disease. Interest in the development of molecules that selectively target α4β2 receptors has been growing, highlighted by the development of the smoking cessation drug, varenicline.[6]

Many have undertaken the task of dissecting nicotinic agonists into a core pharmacophore, since the first publication on the topic in 1970.[10] While the details are debated, two aspects are clear. Nicotinic agonists contain a cationic nitrogen and a hydrogen bond acceptor (**Figure 2.1A**).[11, 12] In 1990, we proposed that binding of the cationic nitrogen of acetylcholine would be mediated through a cation-π interaction with an aromatic residue of the nAChRs.[13] We subsequently validated this model with the identification of a cation-π interaction to a conserved tryptophan residue for both acetylcholine and nicotine.[14, 15] In fact, the cation-π interaction has been shown to be a general contributor to agonist affinity across the entire family of Cys-loop (pentameric) neurotransmitter-gated ion channels.[16]

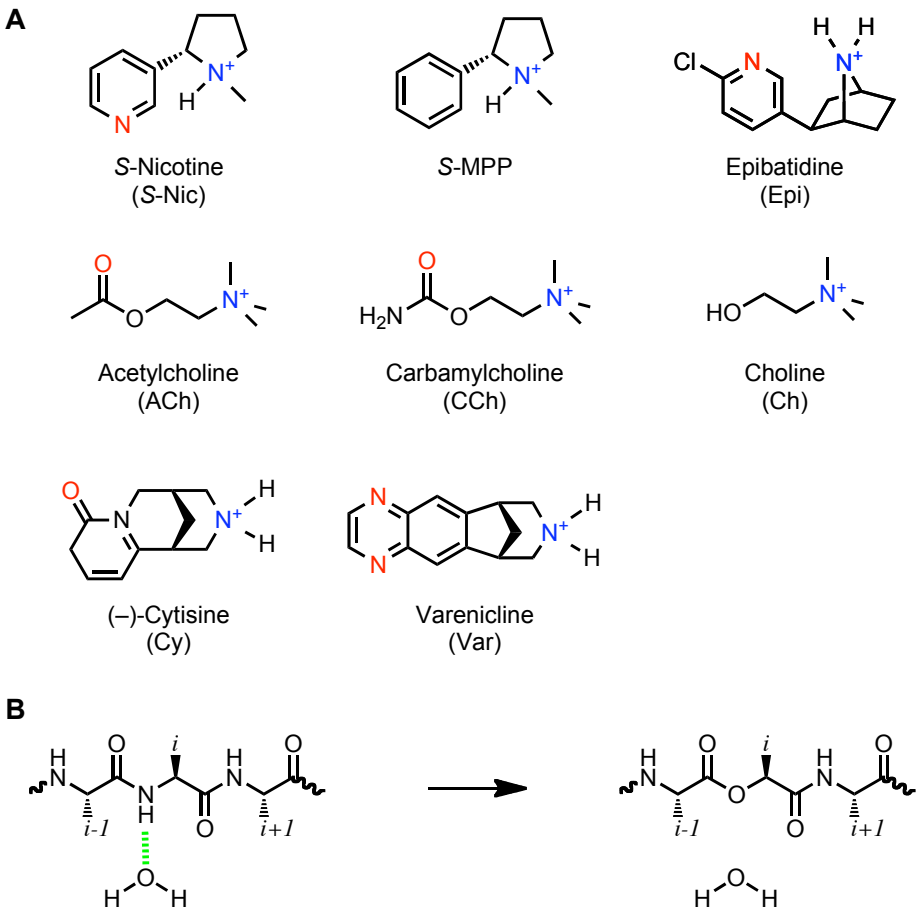

Figure 2.1. Key structures considered in the present work. (A) Structures of agonists used. Hydrogen bond acceptor moieties are red and cationic nitrogens are blue. Cytisine and varenicline are smoking cessation drugs. (B) Backbone amide-to-ester mutation strategy for perturbing a hydrogen bond.

In the nAChRs, ligand binding occurs at the interface between adjacent principal (α4 in α4β2) and complementary (β2) subunits. Three segments from the α4 subunit (historically referred to as the A, B and C "loops") form the principal face of the ligand binding domain, which contains the cation-π binding site, and three segments from the β2 subunit (D, E and F) form the complementary face. A major advance in the study of nAChRs was the discovery of the water-soluble acetylcholine binding proteins (AChBP).[17-22] AChBP serves as a structural template for the extracellular, N-terminal, ligand binding domain of the nAChRs, sharing 20−24% sequence identity with the

ligand-binding domain of the much larger ion channel proteins. Several AChBP structures with ligands bound have been published, including structures of AChBP in complex with the ACh analog carbamylcholine (CCh) and with nicotine[18] and the nicotine analog epibatidine.[21] Drugs that target the nAChR, such as nicotine and epibatidine, typically contain a protonatable amine rather than the quaternary ammonium seen in ACh. Along with the cation-π interaction, the crystallography indicated a hydrogen bond between the N^+H and the backbone carbonyl of the tryptophan that also forms the cation-π interaction, and functional studies on intact receptors confirmed the hydrogen bonding interaction.[14, 23]

Concerning the second component of the pharmacophore, the hydrogen bond acceptor, the AChBP structure produced intriguing results. With nicotine bound, the pyridine nitrogen makes a hydrogen bond to a water molecule that is positioned by hydrogen bonds to the main chains of two residues, the CO of N107 and the NH of L119, both in the complementary subunit (α4β2 numbering; residues are in the β2 sequence FYSNAVVSYDGSIFWLPPA) (**Figure 2.2**).[18] In other structures, including those with CCh or epibatidine bound, the overall binding site structure is preserved, although the key water molecule is not always evident, especially in lower-resolution structures.

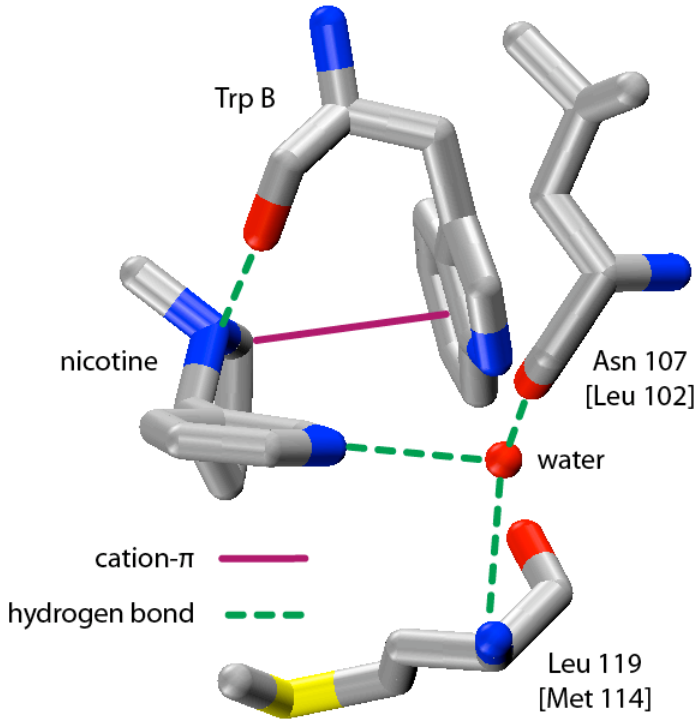

Figure 2.2. Key interactions seen in the crystal structure of nicotine bound to AChBP (pdb: 1UW6). Residue numbering is for the α4β2 receptor, with AChBP homologs in brackets.

A key question, then, is the extent to which predictions based on the AChBPs, which evolved to bind a target molecule, relate to the nAChRs, which evolved to undergo a global structural change (to gate) on binding ACh. Here we describe a novel approach to probe with high precision a specific structural interaction in a complex receptor protein. Using unnatural amino acid mutagenesis and agonist analogs, we find that nicotine, acetylcholine, epibatidine, carbamylcholine and the smoking cessation drug cytisine (the lead compound for the development of varenicline) make the same hydrogen bond to backbone NH of β2L119 in both stoichiometries of the α4β2 receptor, supporting a common pharmacophore for these agonists. Varenicline does not make this interaction and therefore violates the nicotinic pharmacophore.

2.3 RESULTS

2.3.1 General Strategy

A well-established strategy for probing potential backbone hydrogen bonds is to replace the residue that contributes the hydrogen bond donor with its α-hydroxy analog (**Figure 2.1B**).[24-28] This mutation converts a backbone amide to a backbone ester, a subtle change that impacts backbone hydrogen bonding in two ways. The backbone NH that can donate a hydrogen bond is removed, and the carbonyl oxygen, by virtue of being part of an ester rather than an amide, is a weaker hydrogen bond acceptor.

In the present context, simply seeing a change in receptor function in response to appropriate backbone ester substitutions would not prove the presence of the proposed interaction. Backbone mutation is certainly subtle, but when installed in an important region of the receptor it could affect function in a number of ways. As such, we sought a way to provide a direct connection between any consequences of backbone mutation and the proposed hydrogen bond. To do this, we considered the molecule, *S*-*N*-methyl-2-phenylpyrrolidine (*S*-MPP, **Figure 2.1A**). In this structure a phenyl ring replaces the pyridyl group of nicotine, obliterating the possibility of forming the proposed hydrogen bond. This would allow a novel "double mutant cycle" analysis that links the backbone NH to the pyridine N. If the mutant cycle analysis shows that the effects of the two changes – the backbone mutation and the modification of the drug – are substantially non-additive, this would provide compelling evidence for the proposed interaction.

The metric used to evaluate receptors is EC_{50}, the effective concentration of agonist required to achieve half-maximal response. This is a functional measure that can be influenced by changes to drug binding and/or efficacy of activation of the receptor.

Previously we have shown that subtle mutations to TrpB of the binding site primarily, if not exclusively, affect agonist binding,[14] but we cannot assume the same for Leu119. Since the goal here is to map the pharmacophore for a collection of agonists, we are interested in factors that influence receptor activation. We consider EC_{50} to be an appropriately useful guide for understanding agonism and designing new agonists, but more detailed studies of the mutations considered here would be valuable.

2.3.2 Optimization of nonsense suppression experiments

The α4β2 receptor is a pentamer with two possible stoichiometries, $(\alpha4)_2(\beta2)_3$ and $(\alpha4)_3(\beta2)_2$ termed A2B3 and A3B2, respectively. Our initial studies will focus on the A2B3 receptor, which shows the higher sensitivity to nicotine and is thought to be upregulated during chronic nicotine exposure.[29] Later studies will compare the findings for this receptor with those of A3B2. Subunit stoichiometry can be managed by controlling mRNA injection ratios. Exclusive expression of A2B3 or A3B2 can be verified by monitoring I-V relationships of agonist-induced currents, as described previously.[14]

This study represents the first report of unnatural amino acid mutagenesis in the β2 subunit of α4β2. Since nonsense suppression often produces low protein yields of the subunit where the suppression occurs, it was critical to ensure that a receptor with excess β2 subunit, *i.e.*, the A2B3 stoichiometry, was exclusively produced in nonsense suppression experiments. To that end, mRNA ratios substantially favoring the β2 subunit were explored. We found that an injected mRNA ratio of 1:20 of α4:β2 (with β2 containing the nonsense suppression site) gave I-V relationships indicative of A2B3,[14] while still providing enough current to conduct meaningful dose-response experiments. A

10:1 mRNA injection ratio of α4:β2 was sufficient for studies with A3B2. The α4 subunit also contained a known mutation in the M2 transmembrane helix (L9'A), which improves receptor expression and lowers whole-cell EC_{50} values, but does not influence the binding trends of the receptor.[30]

One challenge in incorporating a hydroxy acid at β2L119 was to limit the amount of current observed from oocytes injected with full length tRNA that was not synthetically appended to an amino or α-hydroxy acid. Such current would indicate that the suppressor tRNA was aminoacylated by an endogenous aminoacyl-tRNA synthetase and delivered a natural amino acid at the mutation site. We observed significant background currents attributable to such infidelity when using the suppressor tRNA THG73, which has been the workhorse of our unnatural amino acid mutagenesis experiments[31]. Employing the recently developed opal suppressor tRNA TQOpS' [32, 33] significantly reduced this background current at β2L119. Aminoacylation from TQOpS' was assessed for each agonist by injection of unacylated TQOpS', and full dose-response relations were generated for agonists displaying >20 nA of current. Suppression experiments typically produced ≥1 μA of current and yielded Hill and EC_{50} values that were markedly different from unacylated TQOpS' control experiments, and so the small background currents are not expected to distort the reported EC_{50} values. With these conditions, characterization of mutant receptors was straightforward (**Figure 2.3**).

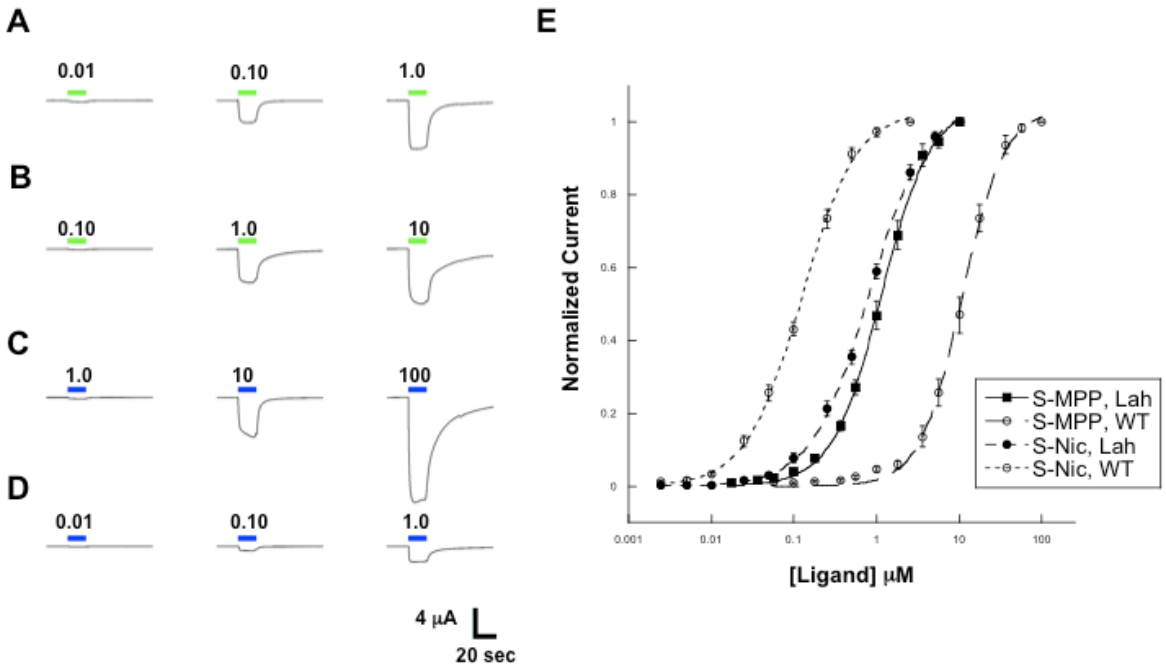

Figure 2.3. Representative current waveforms and dose-response relations for *S*-Nicotine and *S*-MPP at the A2B3 receptor. Agonist-induced current waveforms for (A) *S*-Nicotine on wild-type A2B3. (B) *S*-Nicotine on $(\alpha4)_2(\beta2L119Lah)_3$. (C) *S*-MPP on wild-type A2B3. (D) *S*-MPP on $(\alpha4)_2(\beta2L119Lah)_3$. Concentrations are in μM. (E) Dose-response relations for *S*-Nicotine and *S*-MPP on wild-type A2B3 or $(\alpha4)_2(\beta2L119Lah)_3$.

2.3.3 Amide-to-Ester backbone mutation at β2L119 impacts receptor function in A2B3

To probe the hydrogen bond suggested by the AChBP structures, β2L119 (of A2B3) was replaced with its α-hydroxy analog (leucine, α-hydroxy; Lah). Meaningful increases in EC_{50} for the backbone amide-to-ester mutation were seen for the conventional agonists nicotine, ACh, CCh, and epibatidine, suggesting a significant functional role for the backbone NH (**Table 2.1, Figure 2.3**). In contrast, no shift was seen for the very weak agonist choline.

Table 2.1. EC_{50} values, Hill coefficients, and relative efficacies for mutations to β2L119 in the A2B3 stoichiometry. All studies gave current values at +70 mV (normalized to −110 mV) of ≤0.08, confirming the A2B3 stoichiometry. Errors are standard error of the mean. (±)-Epi is racemic epibatidine. Mutations identified as "Leu" represent recovery of the wild-type receptor by nonsense suppression. The relative efficacy is the ratio of the I_{max} of a saturating concentration of agonist / I_{max} of a saturating concentration of ACh. By definition, the relative efficacy of ACh is 1.

Agonist	Mutation	EC_{50} (nM)	Hill (n_H)	Relative Efficacy
S-Nic	WT	120 ± 5	1.3 ± 0.1	0.27 ± 0.01
	Leu	120 ± 3	1.5 ± 0.1	
	Lah	800 ± 30	1.3 ± 0.1	
S-MPP	WT	11000 ± 400	1.7 ± 0.1	0.23 ± 0.01
	Leu	14000 ± 900	1.5 ± 0.1	
	Lah	1100 ± 40	1.5 ± 0.1	
ACh	WT	360 ± 20	1.3 ± 0.1	[1]
	Leu	440 ± 20	1.3 ± 0.1	
	Lah	3000 ± 100	1.2 ± 0.1	
CCh	WT	7200 ± 80	1.3 ± 0.1	0.50 ± 0.1
	Leu	7900 ± 200	1.2 ± 0.1	
	Lah	29000 ± 800	1.2 ± 0.1	
Ch	WT	140000 ± 4000	1.6 ± 0.1	0.060 ± 0.01
	Leu	140000 ± 20000	1.2 ± 0.1	
	Lah	150000 ± 5000	1.4 ± 0.1	
(±)-Epi	WT	0.79 ± 0.04	1.4 ± 0.1	
	Leu	0.58 ± 0.05	1.5 ± 0.1	0.47 ± 0.03
	Lah	2.9 ± 0.1	1.3 ± 0.1	

As noted above, we considered *S*-MPP as a potentially informative structure for probing the pyridine hydrogen bond. As such, we adapted existing synthetic protocols[34] to prepare *N*-methyl-2-phenylpyrroline (MPP). Recrystallization of the dibenzoyl tartrate salt (at the phenylpyrrolidine stage) gave the *S* enantiomer.

As expected, *S*-MPP is a much poorer agonist than nicotine, showing a ~120-fold higher EC_{50} with the wild-type A2B3 receptor. For nicotine, the *S* enantiomer is the higher affinity enantiomer and the one traditionally used in studies of nicotinic receptors. We find that *S*-MPP has a two-fold lower EC_{50} than racemic MPP, indicating that the higher affinity enantiomer is being used.

Incorporation of a backbone ester at β2L119 leads to a remarkable change in relative agonist potencies. Instead of the increase in EC_{50} seen with nicotine, *S*-MPP

actually shows a *decrease* in EC_{50}; *S*-MPP is a more potent agonist when the backbone ester is present than when the natural backbone amide is present. In fact, when the backbone ester is present, nicotine and *S*-MPP display comparable potency (**Figure 2.3E**).

The AChBP structure also predicts that a second residue in the complementary subunit positions the water molecule in proximity to the pyridine N of nicotine. The backbone carbonyl of β2N107 is expected to make a hydrogen bond to the water molecule in conjunction with the first hydrogen bond made by β2L119 (**Figure 2.2**). As noted above, an established strategy for attenuating the hydrogen bonding ability of a backbone carbonyl is to mutate the (*i+1*) residue to its α-hydroxy acid (**Figure 2.1B**). However, nonsense suppression experiments at the β2A108 site gave inconsistent results that suggested we could not reliably control the stoichiometry of the mutant receptor (**Table 2.2**). As such, we have been unable to successfully probe this interaction.

Table 2.2. EC_{50} values, Hill coefficients, and relative efficacies for mutations to β2A108 in the A2B3 stoichiometry. To confirm stoichiometry, current values at +70 mV (normalized to −110 mV) were determined. In previous studies,[14] we found that a value of ≥0.2 was indicate of the A3B2 stoichiometry and a value of ≤0.08 was indicative of the A2B3 stoichiometry. Note that the current values at +70 mV for "Aah" and "Vah" at this site were consistent with the A3B2 stoichiometry (not the A2B3 stoichiometry we had intended to study) despite the fact that we injected an excess of β2 (up to 100 fold-more than α4). Errors are standard error of the mean. Mutations identified as "Ala" represent recovery of the wild-type receptor by nonsense suppression.

Agonist	Mutation	EC_{50} (nM)	Hill (n_H)	I_{norm} (+70mV)
S-Nic	α4(L9'A)β2	120 ± 10	1.3 ± 0.1	0.05 ± 0.01
	α4(L9'A)β2(A108Ala)	140 ± 10	1.5 ± 0.1	0.07 ± 0.01
	α4(L9'A)β2(A108Aah)	20 ± 10	1.4 ± 0.1	0.40 ± 0.02
	α4(L9'A)β2(A108Val)	50 ± 10	1.1 ± 0.1	0.09 ± 0.06
	α4(L9'A)β2(A108Vah)	50 ± 10	1.1 ± 0.1	0.23 ± 0.03
S-MPP	α4(L9'A)β2	11000 ± 400	1.7 ± 0.1	0.08 ± 0.01
	α4(L9'A)β2(A108Aah)	10000 ± 600	2.0 ± 0.1	0.3 ± 0.03
ACh	α4(L9'A)β2	360 ± 20	1.3 ± 0.1	0.04 ± 0.01
	α4(L9'A)β2(A108Ala)	640 ± 20	1.1 ± 0.1	0.070 ± 0.01
	α4(L9'A)β2(A108Aah)	130 ± 10	1.2 ± 0.1	0.40 ± 0.02
	α4(L9'A)β2(A108Val)	400 ± 10	1.0 ± 0.1	0.090 ± 0.03
	α4(L9'A)β2(A108Vah)	600 ± 50	0.72 ± 0.1	0.2 ± 0.06

2.3.4 Mutant cycle analyses indicate strong receptor-agonist interactions at β2L119 in A2B3

As noted above, a mutant cycle analysis is the standard way to determine whether pairs of mutations are independent or are coupled. EC_{50}-based mutant cycle analyses have been performed by our lab and others to investigate multiple interactions in Cys-loop receptors and related structures[28, 35-37]. For several different agonist pairs, coupling coefficients (Ω) and coupling energies (ΔΔG°) were calculated (**Table 2.3**).

Table 2.3. Coupling parameters (Ω) and ΔΔG° values for mutant cycle analyses for A2B3.

Agonist	Ω	ΔΔG° (kcal/mol)
ACh/Ch	0.16	1.1
CCh/ Ch	0.3	0.71
S-Nic/ *S*-MPP	0.012	2.6

Mutant cycle analysis for the *S*-nicotine/*S*-MPP pair and the β2L119/β2L119Lah pair predicts a substantial coupling energy of 2.6 kcal/mol (**Figure 2.4**). This is a relatively large energy for a putative hydrogen bond, and it provides strong evidence for a hydrogen bonding interaction between the pyridine N of nicotine and the backbone NH of β2L119 in the A2B3 receptor.

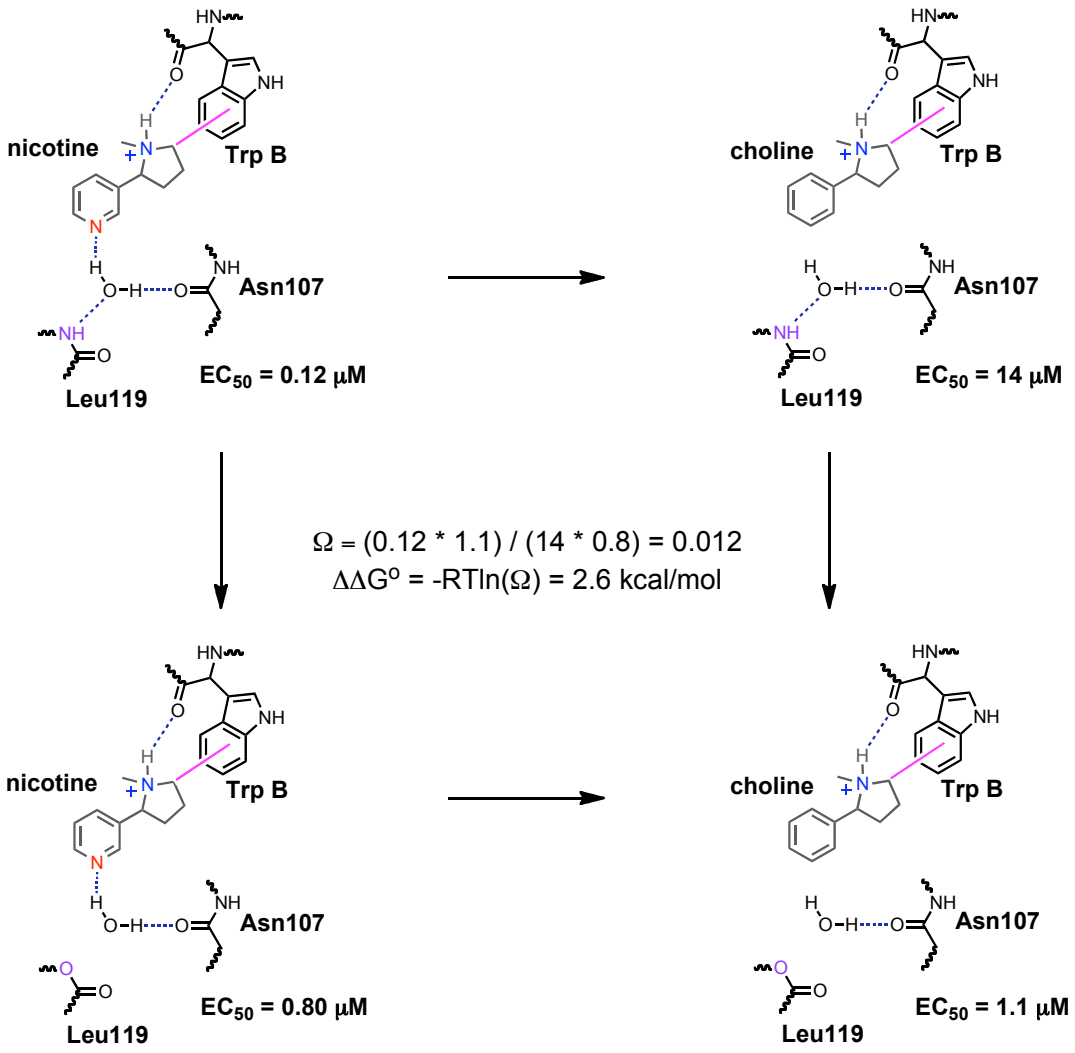

Figure 2.4. Double mutant cycle analysis for *S*-Nic and *S*-MPP on wild-type A2B3 and $(\alpha 4)_2(\beta 2L119Lah)_3$.

We also considered double mutant cycle analyses for the agonists ACh and CCh using choline as the reference compound, as it lacks the key hydrogen bond acceptor. This is a much less subtle probe than the *S*-nicotine/*S*-MPP pair, but it still could produce relevant results. Indeed, we find that for both the ACh/Ch and CCh/Ch pairs, smaller, but still meaningful, coupling energies are seen in the A2B3 receptor (**Table 2.3**).

2.3.5 Studies in the A3B2 subunit stoichiometry give similar results

Recall that the α4β2 receptor can assemble into two different pentameric stoichiometries A2B3 ($(\alpha4)_2(\beta2)_3$) and A3B2 ($(\alpha4)_3(\beta2)_2$). Even though both forms have two agonist binding sites (at appropriate subunit interfaces, shown in **Figure 2.5**), and are both composed of identical α4 and β2 subunits, agonists are generally more potent at the A2B3 stoichiometry (*i.e.*, they give lower EC_{50} values) and this stoichiometry alone is thought to be upregulated during chronic nicotine exposure.[29] We sought to determine whether differences in the pharmacophore binding interactions of the two stoichiometries could account for the differences in receptor pharmacology by evaluating the impact of backbone mutation at β2L119 in A3B2 for ACh and nicotine.

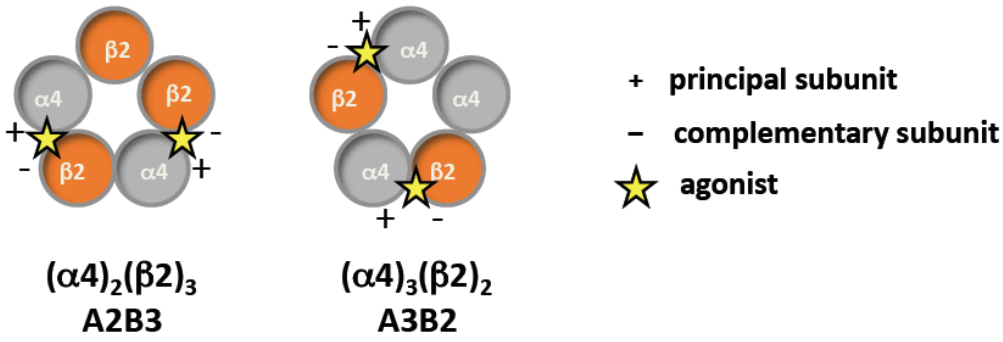

Figure 2.5. Depiction of the two stoichiometries of the α4β2 receptor. Agonist binding sites are depicted at appropriate subunit interfaces.

Note that in all of our studies of the α4β2 receptor (both stoichiometries), we introduce the L9'A mutation[30] to improve receptor expression. Mutations of this type generically increase receptor sensitivity to agonists, and they do so in an additive manner.[38, 39] Thus, in the present study the A3B2 receptors have three L9'A mutations and therefore generally show greater potency than A2B3 receptors, which have two L9'A

mutations, even though the A2B3 stoichiometry is the high affinity form in true wild-type receptors.

For ACh and nicotine, the fold-shifts in EC_{50} in response to the backbone ester mutation at β2L119 in the A3B2 stoichiometry (**Table 2.4**) are comparable to what was seen for the A2B3 stoichiometry (**Table 2.1**). Likewise, agonists lacking a hydrogen bond acceptor displayed similar behavior in the two stoichiometries – no shift in EC_{50} was seen for choline and a large gain of function was seen for *S*-MPP, even larger than the one seen in A2B3.

Table 2.4. EC_{50} values, Hill coefficients, and relative efficacies for mutations to β2L119 in the A3B2 stoichiometry. All studies gave current values at +70 mV (normalized to −110 mV) of ≥0.20, confirming the A3B2 stoichiometry. Errors are standard error of the mean. (±)-Epi is racemic epibatidine. Mutations identified as "Leu" represent recovery of the wild-type receptor by nonsense suppression. The relative efficacy is the ratio of the I_{max} of a saturating concentration of agonist / I_{max} of a saturating concentration of ACh. By definition, the relative efficacy of ACh is 1.

Agonist	Mutation	EC_{50} (nM)	Hill (n_H)	Relative Efficacy
S-Nic	WT	12 ± 0.1	1.6 ± 0.1	0.56 ± 0.04
	Leu	12 ± 0.1	1.6 ± 0.1	
	Lah	67 ± 3	1.4 ± 0.1	
S-MPP	WT	4500 ± 100	1.1 ± 0.1	0.39 ± 0.03
	Leu	4200 ± 300	1.6 ± 0.1	
	Lah	130 ± 10	1.2 ± 0.1	
ACh	WT	26 ± 1	1.1 ± 0.1	[1]
	Leu	26 ± 1	1.6 ± 0.1	
	Lah	220 ± 10	1.2 ± 0.1	
Ch	WT	90000 ± 2000	1.4 ± 0.1	0.70 ± 0.06
	Leu	76000 ± 200	1.4 ± 0.1	
	Lah	74000 ± 2000	1.5 ± 0.1	

Mutant cycle analyses of the ACh/Ch and *S*-Nic/*S*-MPP pairs gave strong energetic couplings of 1.3 and 3.1 kcal/mol, respectively (**Table 2.5**). These values are comparable to what was seen in the A2B3 stoichiometry, suggesting that the hydrogen bond to β2L119 does not differentiate the two subunit stoichiometries.

Table 2.5. Coupling parameters (Ω) and ΔΔG° values for mutant cycle analyses in A3B2.

Agonist	Ω	ΔΔG° (kcal/mol)
ACh/Ch	0.12	1.3
S-Nic/*S*-MPP	0.0055	3.1

2.3.6 Studies with smoking cessation drugs at both subunit stoichiometries

We also evaluated whether two established smoking cessation compounds (**Figure 2.1A**) are sensitive to the amide-to-ester mutation at β2L119. Varenicline (marketed by Pfizer as Chantix® in the U.S.) was designed to target α4β2 receptors, and was approved for use as a smoking cessation aid in 2006.[6] Cytisine is a naturally occurring alkaloid that served as a lead compound for the development of varenicline. It is marketed for smoking cessation in Eastern Europe as Tabex®, although compelling clinical trials that establish its effectiveness have not been published.[40]

Our results for varenicline are surprising (**Table 2.6)**. With only a 2-fold shift in A2B3 and no meaningful shift in A3B2, it would appear that there is no hydrogen bond between a quinoxaline N of varenicline and the backbone NH of β2L119 in the α4β2 receptor. With the exception of choline (which does not contain the hydrogen bond acceptor), this is the only agonist that we have found to be insensitive to this mutation.

Table 2.6. EC_{50} values, Hill coefficients, and relative efficacies for (−)-cytisine and varenicline at both subunit stoichiometries. All studies gave current values at +70 mV (normalized to −110 mV) of ≤0.08 or ≥0.20, confirming the A2B3 and A3B2 stoichiometries, respectively. Errors are standard error of the mean. Cy is (−)-cytisine and Var is varenicline. Mutations identified as "Leu" represent recovery of the wild-type receptor by nonsense suppression. The relative efficacy is the ratio of the I_{max} of a saturating concentration of agonist / I_{max} of a saturating concentration of ACh.

Agonist	Mutation	EC_{50} (nM)	Hill (n_H)	Relative Efficacy
		A2B3 Stoichiometry		
Cy	WT	6.9 ± 0.3	1.4 ± 0.1	0.030 ± 0.01
	Leu	8.7 ± 0.4	1.2 ± 0.1	
	Lah	540 ± 30	0.98 ± 0.1	
Var	WT	3.1 ± 0.1	1.4 ± 0.1	0.12 ± 0.02
	Leu	2.6 ± 0.2	1.3 ± 0.1	
	Lah	4.7 ± 0.2	1.3 ± 0.1	
		A3B2 Stoichiometry		
Cy	WT	3.1 ± 0.1	1.9 ± 0.1	0.54 ± 0.05
	Leu	3.6 ± 0.1	1.9 ± 0.1	
	Lah	51 ± 2	1.4 ± 0.1	
Var	WT	0.95 ± 0.02	1.7 ± 0.1	0.33 ± 0.01
	Leu	1.0 ± 0.1	1.5 ± 0.1	
	Lah	1.1 ± 0.1	1.2 ± 0.1	

Cytisine also produces intriguing results. A remarkable 62-fold shift is seen for this subtle backbone ester mutation in the A2B3 receptor. This is among the strongest effects we have ever seen for a backbone ester mutation in any protein. A much smaller effect is seen in the A3B2 receptor, although it is still larger than what is seen for any other drug/receptor combination for mutation at β2L119.

2.4 DISCUSSION

The nicotinic receptor has produced one of the longest-known, best-studied pharmacophores. The original study of Beers and Reich[10] proposed that two points, a cationic nitrogen and a hydrogen bond acceptor, were required for successful interaction with biological receptors. Later discussion debated the optimal distance between the two points (deemed the "internitrogen distance"), and more recent models have alluded to pharmacophore binding partners within the biological receptors. Despite 40 years of interest in the nicotinic pharmacophore, the binding partners of the essential two point

pharmacophore have only recently been identified. Pioneering mutagenesis and affinity labeling studies of the receptor from *Torpedo* rays identified a number of aromatic amino acids near the binding site.[1, 3] Early unnatural amino acid mutagenesis studies showed that one of these aromatics, now termed TrpB, makes a cation-π interaction with ACh in the muscle-type nAChR,[15] and more recent studies established a comparable interaction to both ACh and nicotine in the α4β2 receptor.[14]

The search for the presumed hydrogen bond donor to the acetyl group of ACh and the pyridine N of nicotine was much more challenging. A breakthrough came with the discovery of the AChBPs, and in 2004 a structure of nicotine bound to AChBP was reported.[18] As shown in **Figure 2.2**, that AChBP structure confirmed the cation-π interaction to TrpB. It also implicated a hydrogen bond between the pyrrolidine N^+H and the backbone carbonyl of TrpB, an interaction that was subsequently confirmed by unnatural amino acid mutagenesis.[14, 23]

Importantly, the AChBP structure also suggested the binding partner for the second element of the pharmacophore. In AChBP, the pyridine N of nicotine makes a water-mediated hydrogen bond to a backbone NH and to a backbone carbonyl (**Figure 2.2**). This elegant arrangement emphasizes the interfacial nature of the agonist binding site, as the pyridine N interacts with residues that are on the complementary subunit, while TrpB, which makes the cation-π interaction and the hydrogen bond to the pyrrolidine N^+H, lies in the principal subunit. The value of AChBP in guiding nAChR research is undeniably large, especially in the present context. It would have been very challenging to guess the hydrogen bond partner(s) to agonists such as ACh and nicotine before the structure of AChBP with nicotine bound. Nevertheless, AChBP is not a

nAChR. AChBP evolved to bind ligands, not to gate an ion channel in response to ACh binding. As such, tests of predictions from AChBP structures in real receptors are always essential.

Here we employ a novel strategy to test the water-mediated hydrogen bonding model of **Figure 2.2** in the neuronal, α4β2 nAChR. The α4β2 receptor shows high affinity for nicotine, and it is generally accepted to be the dominant receptor subtype that contributes to nicotine addiction. Our studies of α4β2 are made possible by recent advances[14] that allow us to express significant quantities of α4β2 in *Xenopus* oocytes, to control subunit stoichiometry, and to efficiently incorporate unnatural amino acids into the receptor. Recently, we have shown that the cation-π interaction and the hydrogen bond to TrpB are strong in the A2B3 receptor.[14]

To probe the second hydrogen bond suggested by AChBP, we mutated β2L119 to its α-hydroxy analog. This removes the critical NH, and, indeed, the agonists nicotine, ACh, CCh, and epibatidine all show 5−7-fold increases in EC_{50} in response to the mutation in the A2B3 stoichiometry. While consistent with the hydrogen bonding model, these observations certainly do not prove it. It could be that the backbone mutation is simply generically disruptive to receptor function.

To make an explicit connection between the pyridine N of nicotine and the backbone NH of β2L119, we combined backbone mutagenesis with a modification of the agonist, removing the pyridine N to create *S*-MPP. Of course, *S*-MPP would never be the target of a medicinal chemistry study; it can be anticipated to be a terrible drug at the nAChR. Here it is used as a chemical probe, to evaluate a key binding interaction of the potent drug nicotine.

Studies with *S*-MPP produced remarkable results. As expected, it is a very poor agonist at the wild-type receptor. However, completely opposite to what is seen with nicotine, ACh, or epibatidine, introduction of the backbone ester at β2L119 *lowers* EC_{50} for *S*-MPP in the A2B3 stoichiometry. In fact, *S*-MPP and nicotine are comparably potent at the mutant receptor (**Figure 2.3E**). Clearly the backbone mutation has had dramatically different effects on the two agonists. The effect can be quantified by a mutant cycle analysis, which reveals a coupling energy of 2.6 kcal/mol between the backbone mutation and the agonist "mutation." This is a quite substantial energy, especially when one considers that these chemical changes – both in the protein and in the ligand – are more structurally subtle than those typically employed in mutant cycle analysis studies using conventional mutagenesis.

The results with *S*-MPP provide strong support for the nicotine binding model based on the AChBP structure. As noted above, however, AChBP structures with CCh or epibatidine bound do not include the key water molecule, although other components of the hydrogen bonding network are comparably positioned. We find that ACh, CCh, and epibatidine all respond to the backbone ester mutation in a way that is comparable to that seen for nicotine. In addition, choline, a weak agonist that lacks the hydrogen bond acceptor of ACh and CCh, is not influenced by the backbone mutation. We thus conclude that all the drugs studied here (with the exception of varenicline as discussed below) make a hydrogen bonding interaction with the backbone NH of β2L119; the nicotinic pharmacophore has thus been completed by interactions with the complementary subunit. Note that these studies do not establish that the interaction between the hydrogen bond acceptor component of the agonists and the backbone NH of

β2L119 is mediated by a water molecule; a direct interaction would be just as compatible with our data. At present, we feel the water-mediated interaction is the most reasonable interpretation, but further experiments to address this point would be valuable.

Nearly identical responses to the amide-to-ester mutation at β2L119 were seen in the A3B2 stoichiometry for ACh, nicotine, choline, and *S*-MPP, suggesting that this hydrogen bonding interaction is present in both receptor stoichiometries. Other studies in our lab have shown that ACh and nicotine are also equivalently sensitive to perturbations of the other binding interaction of the pharmacophore – the cation-π interaction to TrpB and the hydrogen bond to the backbone CO of TrpB. As such, it is still a mystery as to why the two stoichiometries have vastly different agonist affinities given that they both have two agonist binding sites composed of identical subunits. It is possible that the accessory subunit – the fifth subunit that does not participate in a binding interface, an α4 in A3B2 and β2 in A2B3 – makes the difference.

The two smoking cessation compounds, varenicline and cytisine, show interesting variations with regard to the backbone ester mutation. Varenicline is qualitatively different from all the other compounds considered here. With a minimal (<2-fold) effect at the A2B3 stoichiometry and no meaningful effect at the A3B2 stoichiometry, we conclude that varenicline violates the nicotinic pharmacophore and does not make a hydrogen bond to the backbone NH of L119 in the β2 subunit. **Figure 2.6** provides a rationalization. By visual inspection, and from the distances shown, it is clear that the quinoxaline nitrogens of varenicline are not well aligned with the hydrogen bond acceptor moieties of nicotine and varenicline, and so they cannot hydrogen bond to L119. While medicinal chemists and pharmacologists familiar with this system may have

anticipated this result, experimental confirmation of expectations from modeling is always valuable.

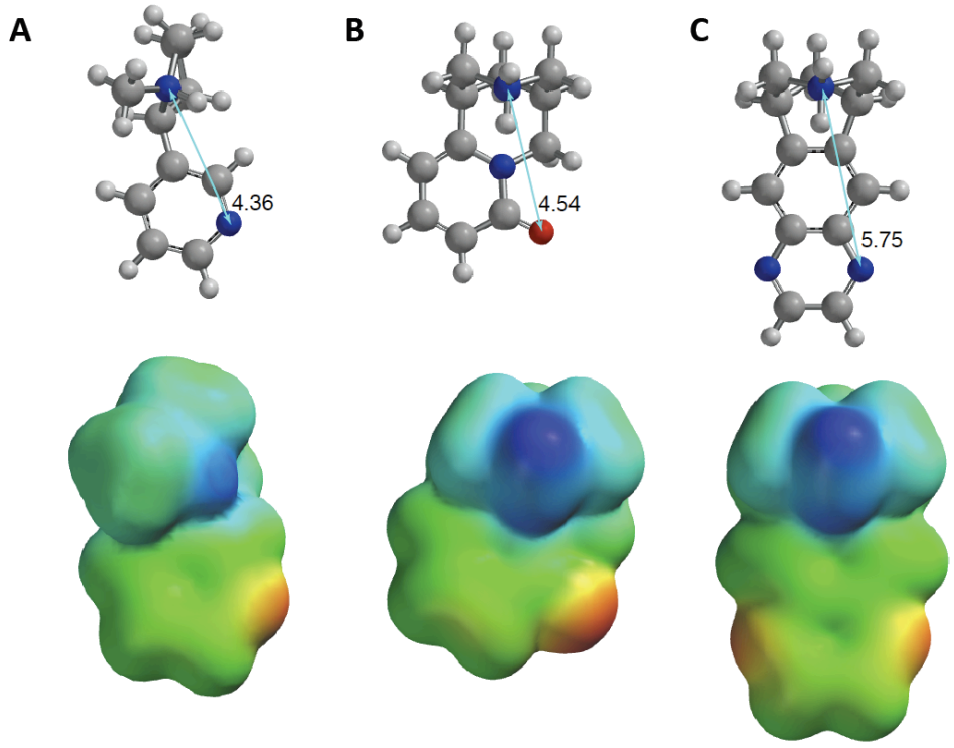

Figure 2.6. "Internitrogen distances" and electrostatic potential maps (as calculated in Spartan) for (A) *S*-nicotine, (B) (−)-cytisine and (C) varenicline. Geometries were optimized at RHF-3-21G*. The electrostatic potential map range is −20 to +700. The molecule ranges are: nicotine = +27 to +658; cytisine −18 to +701; and varenicline +35 to +691.

Cytisine shows an intriguing hydrogen bonding pattern, distinct from the other agonists considered here. More so than the other drugs, cytisine shows a strong stoichiometry selectivity in the α4β2 receptor, having a much greater efficacy at the A3B2 stoichiometry than at the A2B3. Interestingly, cytisine also shows the greatest stoichiometry differences for the amide-to-ester mutation. The A2B3 stoichiometry shows a remarkable 62-fold rise in EC_{50}, much larger than anything we have seen previously. The A3B2 stoichiometry shows a much smaller effect.

Despite these differences, cytisine shows the strongest sensitivity to backbone ester mutation of any of the agonists tested at both stoichiometries. We can rationalize this general effect with reference to the electrostatic potential plots of **Figure 2.6**. Visually, the carbonyl oxygen of cytisine presents a much stronger negative electrostatic potential than the corresponding nitrogen of nicotine. Quantitative evaluation of the electrostatic potentials at these atoms confirms the visual. Thus, the oxygen of cytisine should be a better hydrogen bond acceptor than the nitrogen of nicotine, completely consistent with expectation for an amide carbonyl *vs*. a pyridine nitrogen.

We have now used chemical-scale investigations of functional receptors to establish a three-point interaction between nicotine and the α4β2 neuronal nAChR, the receptor most strongly associated with nicotine addiction. A cation-π interaction to TrpB has been established by progressive fluorination of the key tryptophan. Backbone mutagenesis has been used to establish two key hydrogen bonds: the pyrrolidine N^+H hydrogen bonds to the backbone carbonyl of TrpB, and the pyridine N of nicotine hydrogen bonds to the backbone NH of β2L119. Studies of these two hydrogen bonds were inspired by the AChBP structures, emphasizing the substantial impact of AChBP on nAChR research.

At the same time, AChBP is not a neurotransmitter-gated ion channel; it evolved to serve a different function than a nAChR. As such, we should anticipate some differences between the two structures. Indeed, two features of the nicotine-AChBP structure have been shown to be not functionally significant in studies of nAChRs. The AChBP structure clearly shows a cation-π interaction between the CH_3 of nicotine and a tyrosine at the agonist binding site termed TyrC2 (**Figure 2.7**).[18] This methyl group –

which carries a charge comparable to a CH_3 attached to the N^+ of ACh, points directly at the center of the aromatic ring of TyrC2 and essentially makes van der Waals contact with the ring, unquestionably a cation-π interaction. However, we find no experimental support for this cation-π interaction in either the muscle-type or the α4β2 nAChR. In each system, inserting 4-CN-Phe at TyrC2 gives essentially wild-type receptor function.[14, 15] A CN group is very strongly deactivating in a cation-π interaction, and so this result is in conflict with the AChBP structure. Note that in a different Cys-loop receptor, the residue at position C2 does make a functionally significant cation-π interaction to the natural agonist serotonin.[41] Also, in the neuronal α7 receptor, epibatidine (but not ACh) has been recently shown to make a cation-π interaction with the C2 tyrosine.[42]

In addition, all AChBP structures – the nicotine, CCh, and epibatidine bound structures considered here as well as the "apo" structure – contain a strong hydrogen bond between the indole NH of TrpB and the backbone carbonyl of the residue that corresponds to β2L119 (**Figure 2.7**). N•••O distances range from 2.7 to 3.0 Å. However, earlier studies of the muscle-type receptor found no evidence for an important interaction of this kind. In particular, TrpB can be substituted by unnatural amino acids in which the indole ring is replaced by a naphthalene or an *N*-methylindole with very little impact on EC_{50}.[15] All of these analogs lack the critical hydrogen bond-donating NH of the Trp indole ring.

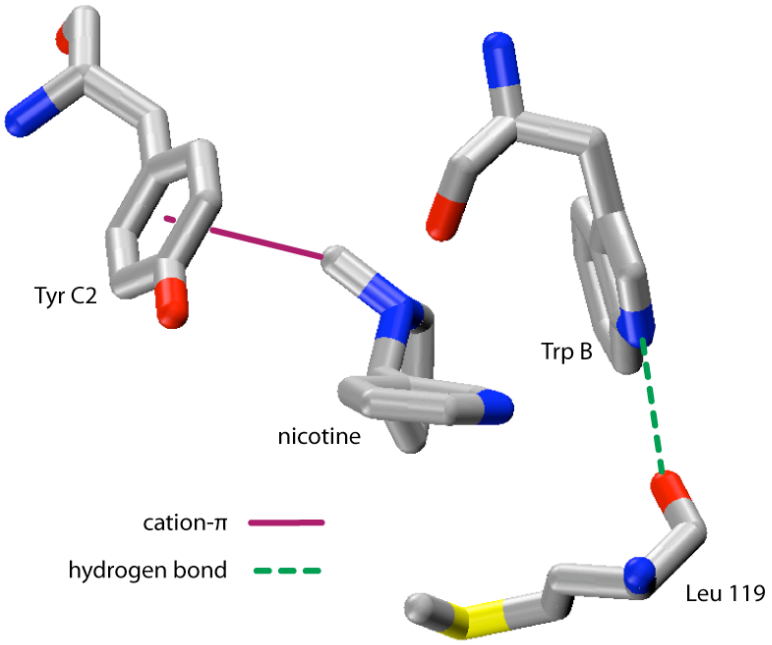

Figure 2.7. Additional interactions seen in the crystal structure of nicotine bound to AChBP (pdb: 1UW6). Residue numbering is for the α4β2 receptor.

In summary, we have used a combination of unnatural amino acid mutagenesis and chemical synthesis to provide strong evidence for a functionally important hydrogen bond between the pyridine N of nicotine and the backbone NH of β2L119 in the nicotine-sensitive α4β2 receptor at both subunit stoichiometries. A similar interaction contributes to the binding of ACh, CCh, epibatidine, and cytisine, but not to the binding of the popular smoking cessation drug, varenicline. We have now used unnatural amino acid mutagenesis to establish three strong contact points between this critical receptor and nicotine: the cation-π interaction to the side chain of TrpB; the hydrogen bond between the pyrrolidine $N^{+}H$ and the backbone carbonyl of TrpB; and the hydrogen bond between the pyridine N and the backbone NH of β2L119. There is much interest in the pharmaceutical industry in developing subtype-selective agonists of neuronal nAChRs, and it seems likely that the complementary subunit will play the dominant role in

discriminating among subtypes. As such, these studies of a key binding interaction involving the complementary binding site suggest a general strategy for developing insights that could lead to subtype-specific pharmaceuticals.

2.5 EXPERIMENTAL SECTION

Rat α4 and β2 cDNA in the pAMV vector was linearized with the restriction enzyme Not 1. mRNA was prepared by *in vitro* transcription using the mMessage Machine T7 kit (Ambion). Unnatural mutations were introduced by the standard Stratagene QuickChange protocol, using a TGA mutation at the site of interest. The α4 subunit contained a known mutation in the M2 transmembrane helix (L9'A) that improves receptor expression and lowers whole-cell EC_{50} values, but does not influence the ligand-binding trends of the receptor.[30] Stage V-VI *Xenopus laevis* oocytes were injected with mRNA in α4L9'A:β2 ratio of 1:1 for wild-type experiments, 1:20 for suppression in A2B3 and 10:1 for suppression in A3B2. Hydroxy or amino acids were appended to the dinucleotide dCA and enzymatically ligated to the truncated 74-nucleotide TQOpS' tRNA as previously described.[31] Each cell was injected with 75 nL of a 1:1 mixture of mRNA (20-25 ng of total mRNA): tRNA (20-30 ng), with oocytes injected with Leu ligated to TQOpS' receiving an additional 75 nL after 24 hrs of incubation at 18 °C. Wild-type recovery experiments (injection of tRNA appended to the natural amino acid) were preformed to evaluate the fidelity of the unnatural suppression experiments. Additional controls, mRNA only and 74-mer TQOpS' ligated to dCA (TQOpS'-dCA), were also examined. While small currents (typically less than 200 nA) were seen for TQOpS'-dCA control experiments, EC_{50} and Hill values were substantially different from suppression values.

Electrophysiology experiments were performed 24-48 hrs after injection using the OpusXpress 6000A instrument (Axon Instruments) in two-electrode voltage clamp mode at a holding potential of −60 mV. The running buffer was Ca^{2+} free ND96 solution (96 mM NaCl, 2 mM KCl, 1 mM $MgCl_2$, and 5 mM HEPES, pH 7.5). During typical recordings, agonists were applied for 15 s followed by a 116 s wash with the running buffer. For recordings with epibatidine, cytisine and varenicline, the first 8 drug concentrations were applied for 90 s with a 116 s wash with running buffer, while the remaining concentrations were applied for 15 s with a 116 s wash. Dose-response data were obtained for ≥8 agonist concentrations on ≥6 cells. All EC_{50} and Hill coefficient values were obtained by fitting dose-response relations to the Hill equation and are reported as averages ± standard error of the fit. A detailed error analysis of nonsense suppression experiments reveals data are reproducible to ±50% in EC_{50}.[43, 44] Voltage jump experiments were conducted to verify stoichiometry as described previously.[14]

Double mutant cycle analyses were performed with EC_{50} values to calculate coupling coefficients (Ω) using the equation: $\Omega = (EC_{50}^{\text{Leu, ligand}} * EC_{50}^{\text{Lah, ligand analog}})/(EC_{50}^{\text{Leu, ligand analog}} * EC_{50}^{\text{Lah, ligand}})$, where [Leu, ligand] and [Leu, ligand analog] represent the EC_{50} of the wild-type receptor with either ligand and [Lah, ligand] and [Lah, ligand analog] represent the EC_{50} of the ester mutation with either ligand. Coupling energies, $\Delta\Delta G°_{int}$, were calculated from the equation $\Delta\Delta G°_{int} = -RT\ln\Omega$.

Synthesis of *N*-methyl-2-phenylpyrrolidine hydrochloride. 2-phenylpyrrolidine (5.0 g, 34 mmol), prepared according to a published protocol,[34] was mixed with dibenzoyl-*L*-tartatric acid (6.1 g, 17 mmol) in a 100 mL round-bottom flask equipped with a reflux condenser. To this was added 35% ethanol in ethylacetate (30 mL). The solution was

heated to boiling for 10 minutes and then cooled to room temperature overnight. The white crystals were collected, rinsed with cold ethylacetate and then submitted to five sequential recrystallizations. Yield (10%, 2.2 g). ^{1}H NMR ($CDCl_3$, 300 MHz) δ 8.20 (4H, m), 7.61-7.32 (16H, m), 5.92 (2H, s), 5.03 (4H, b), 4.54 (2H, dd, *J* = 9.1, 6.7 Hz), 3.38 (4H, m), 2.27–2.00 (8H, m); ^{13}C NMR ($CDCl_3$, 75 MHz) δ 172.58, 166.45, 134.91, 132.73, 130.54, 129.70, 128.83, 128.76, 128.03, 127.37, 75.60, 62.74, 44.80, 30.42, 23.37. HRMS (FAB+) *m/z* calc'd for $C_{10}H_{14}N$ [M+]: 148.1126, found 148.1081. To obtain enantioenriched 2-phenylpyrrolidine, the product was vigorously stirred in a 1:1 mixture of 2 M NaOH: CH_2Cl_2. The organic layer was then extracted with additional CH_2Cl_2 (3×), washed with brine, dried over Na_2SO_4, and concentrated to yield enantioenriched 2-phenylpyrrolidine as a yellow oil (Yield: 95%). NMR spectra are consistent with previously reported data. HRMS (FAB+) *m/z* calc'd for $C_{10}H_{14}N$ [M+H]: 148.1126, found 148.1134. To establish enantiomeric excess, the product was converted to ethyl 2-phenylpyrrolidine-1-carboxylate via a previously described procedure,[45] and this material was evaluated by analytical chiral HPLC analysis using a Chiralcel OD-H column (4.6 mm × 25 cm) from Daicel Chemical Industries, Ltd. with 2% isopropyl alcohol in hexanes, giving an enantiomeric excess of 96%. ^{1}H NMR of ethyl 2-phenylpyrrolidine-1-carboxylate (CH_3OD, 300 MHz) δ 7.32-7.15 (5H, m), 4.92 (1H, m), 4.08 (IH, m), 3.92 (1H, m), 3.59 (2H, q, *J* = 7.7 Hz), 2.34 (1H, m), 1.95–1.86 (4H, m), 1.26 (1H, t, *J* = 7.0 Hz), 0.94 (1H, t, *J* = 7Hz); ^{13}C NMR of ethyl 2-phenylpyrrolidine-1-carboxylate ($CDCl_3$, 75 MHz) δ 155.40, 144.32, 128.22, 126.59, 125.44, 60.85, 47.34, 47.03, 35.71, 23.58, 14.79. HRMS of ethyl 2-phenylpyrrolidine-1-carboxylate (FAB+) *m/z* calc'd for $C_{13}H_{18}O_2N$ [M+H]: 220.1338, found 220.1336.

Enantioenriched 2-phenylpyrrolidine from above, (0.13 g, 0.86 mmol) was added to a two-neck, 25 mL round-bottom flask equipped with a reflux condenser. To this was added 4 mL of formic acid and 2 mL of 37 wt% formaldehyde (in H_2O). The mixture was stirred and heated to reflux at 80 °C for 3 hrs. The solution was cooled to room temperature and made basic (pH 12) by the addition of 2M NaOH. The organics were extracted with CH_2Cl_2, washed with brine, dried over Na_2SO_4 and concentrated. The resulting yellow oil was placed into a 25 mL round-bottom flask and dissolved in 5 mL of cold ether. HCl (g) was generated and passed into the solution by slow addition of HCl (aq, 12 M) into H_2SO_4 (aq) The resulting white crystals were collected by filtration and dried. Yield: 83%, 140 mg. $[\alpha]^{24}{}_D = -110°$ (c = 1, $CHCl_3$); ^{1}H NMR ($CDCl_3$, 300 MHz) δ 7.66 (2H, m), 7.32 (3H, m), 4.14 (1H, m), 3.95 (1H, b), 3.05 (2H, m), 2.60 (3H, d, *J* = 4.7 Hz), 2.29 (4H, m); ^{13}C NMR ($CDCl_3$, 75 MHz) δ 131.99, 129.89, 129.31, 128.76, 73.05, 44.43, 37.67, 31.94, 20.95; HRMS (FAB+) *m/z* calc'd for $C_{11}H_{16}N$ [M+]: 162.1283, found 162.1325.

2.6 ACKNOWLEDGEMENTS

We thank Ariele P. Hanek and Sean M. A. Kedrowski for helpful discussions. This work was supported by the NIH (NS 34407; NS 11756) and the California Tobacco-Related Disease Research Program of the University of California, grant number 16RT-0160. Varenicline tartrate was a generous gift from Targacept.

2.7 REFERENCES

1. Corringer, P. J.; Le Novere, N.; Changeux, J. P., Nicotinic receptors at the amino acid level. *Annu. Rev. Pharmacol. Toxicol.* **2000,** 40, 431-58.
2. Grutter, T.; Changeux, J. P., Nicotinic receptors in wonderland. *Trends Biochem. Sci.* **2001,** 26, (8), 459-63.
3. Karlin, A., Emerging structure of the nicotinic acetylcholine receptors. *Nat. Rev. Neurosci.* **2002,** 3, (2), 102-14.
4. Gotti, C.; Zoli, M.; Clementi, F., Brain nicotinic acetylcholine receptors: native subtypes and their relevance. *Trends Pharmacol. Sci.* **2006,** 27, (9), 482-91.
5. Romanelli, M. N.; Gratteri, P.; Guandalini, L.; Martini, E.; Bonaccini, C.; Gualtieri, F., Central nicotinic receptors: structure, function, ligands, and therapeutic potential. *ChemMedChem* **2007,** 2, (6), 746-67.
6. Coe, J. W.; Brooks, P. R.; Vetelino, M. G.; Wirtz, M. C.; Arnold, E. P.; Huang, J.; Sands, S. B.; Davis, T. I.; Lebel, L. A.; Fox, C. B.; Shrikhande, A.; Heym, J. H.; Schaeffer, E.; Rollema, H.; Lu, Y.; Mansbach, R. S.; Chambers, L. K.; Rovetti, C. C.; Schulz, D. W.; Tingley, F. D., 3rd; O'Neill, B. T., Varenicline: an alpha4beta2 nicotinic receptor partial agonist for smoking cessation. *J. Med. Chem.* **2005,** 48, (10), 3474-7.
7. Mansvelder, H. D.; Keath, J. R.; McGehee, D. S., Synaptic mechanisms underlie nicotine-induced excitability of brain reward areas. *Neuron* **2002,** 33, (6), 905-19.
8. Nashmi, R.; Xiao, C.; Deshpande, P.; McKinney, S.; Grady, S. R.; Whiteaker, P.; Huang, Q.; McClure-Begley, T.; Lindstrom, J. M.; Labarca, C.; Collins, A. C.; Marks, M. J.; Lester, H. A., Chronic nicotine cell specifically upregulates functional alpha4 nicotinic receptors: basis for both tolerance in midbrain and enhanced long-term potentiation in perforant path. *J. Neurosci.* **2007,** 27, (31), 8202-18.
9. Tapper, A.; McKinney, S.; Nashmi, R.; Schwarz, J.; Deshpande, P.; Labarca, C.; Whiteaker, P.; Collins, A.; Lester, H., Nicotine activation of alpha4 receptors: sufficient for reward, tolerance and sensitization. *Science* **2004,** 306, 1029-1032.
10. Beers, W. H.; Reich, E., Structure and activity of acetylcholine. *Nature* **1970,** 228, (5275), 917-22.
11. Glennon, R. A.; Dukat, M., Central nicotinic receptor ligands and pharmacophores. *Pharm. Acta. Helv.* **2000,** 74, (2-3), 103-14.
12. Glennon, R. A.; Dukat, M.; Liao, L., Musings on alpha4beta2 nicotinic acetylcholine (nACh) receptor pharmacophore models. *Curr. Top. Med. Chem.* **2004,** 4, (6), 631-44.
13. Dougherty, D. A.; Stauffer, D. A., Acetylcholine binding by a synthetic receptor. Implications for biological recognition. *Science* **1990,** 250, 1558-1560.
14. Xiu, X.; Puskar, N. L.; Shanata, J. A.; Lester, H. A.; Dougherty, D. A., Nicotine binding to brain receptors requires a strong cation-π interaction. *Nature* **2009,** 458, (7237), 534-7.
15. Zhong, W.; Gallivan, J.; Zhang, Y.; Li, L.; Lester, H.; Dougherty, D., From *ab initio* quantum mechanics to molecular neurobiology: A cation-π binding site in the nicotinic receptor. *Proc. Natl. Acad. Sci. USA* **1998,** 95, 12088-12093.

16. Dougherty, D. A., Cys-loop neuroreceptors: Structure to the rescue? *Chem. Rev.* **2008,** 108, (5), 1642-1653.
17. Brejc, K.; van Dijk, W. J.; Klaassen, R. V.; Schuurmans, M.; van Der Oost, J.; Smit, A. B.; Sixma, T. K., Crystal structure of an ACh-binding protein reveals the ligand-binding domain of nicotinic receptors. *Nature* **2001,** 411, (6835), 269-76.
18. Celie, P.; van Rossum-Fikkert, S.; Van Dyke, W.; Brejc, K.; Smit, A.; Sixma, T., Nicotine and carbamylcholine binding to nicotinic acetylcholine receptors as studied in AChBP crystal structures. *Neuron* **2004,** 41, 907-914.
19. Rucktooa, P.; Smit, A. B.; Sixma, T. K., Insight in nAChR subtype selectivity from AChBP crystal structures. *Biochem. Pharmacol.* **2009,** 78, (7), 777-87.
20. Hansen, S. B.; Sulzenbacher, G.; Huxford, T.; Marchot, P.; Bourne, Y.; Taylor, P., Structural characterization of agonist and antagonist-bound acetylcholine-binding protein from *Aplysia californica*. *J. Mol. Neurosci.* **2006,** 30, (1-2), 101-2.
21. Hansen, S. B.; Sulzenbacher, G.; Huxford, T.; Marchot, P.; Taylor, P.; Bourne, Y., Structures of Aplysia AChBP complexes with nicotinic agonists and antagonists reveal distinctive binding interfaces and conformations. *EMBO J.* **2005,** 24, (20), 3635-46.
22. Taylor, P.; Talley, T. T.; Radic, Z.; Hansen, S. B.; Hibbs, R. E.; Shi, J., Structure-guided drug design: conferring selectivity among neuronal nicotinic receptor and acetylcholine-binding protein subtypes. *Biochem. Pharmacol.* **2007,** 74, (8), 1164-71.
23. Cashin, A. L.; Petersson, E. J.; Lester, H. A.; Dougherty, D. A., Using physical chemistry to differentiate nicotinic from cholinergic agonists at the nicotinic acetylcholine receptor. *J. Am. Chem. Soc.* **2005,** 127, (1), 350-356.
24. Koh, J. T.; Cornish, V. W.; Schultz, P. G., An experimental approach to evaluating the role of backbone interactions in proteins using unnatural amino acid mutagenesis. *Biochemistry* **1997,** 36, 11314-11322.
25. England, P. M.; Zhang, Y. N.; Dougherty, D. A.; Lester, H. A., Backbone mutations in transmembrane domains of a ligand-gated ion channel: Implications for the mechanism of gating. *Cell* **1999,** 96, (1), 89-98.
26. Deechongkit, S.; Dawson, P. E.; Kelly, J. W., Toward assessing the position-dependent contributions of backbone hydrogen bonding to beta-sheet folding thermodynamics employing amide-to-ester perturbations. *J. Am. Chem. Soc.* **2004,** 126, (51), 16762-71.
27. Deechongkit, S.; Nguyen, H.; Powers, E. T.; Dawson, P. E.; Gruebele, M.; Kelly, J. W., Context-dependent contributions of backbone hydrogen bonding to beta-sheet folding energetics. *Nature* **2004,** 430, (6995), 101-5.
28. Gleitsman, K. R.; Kedrowski, S. M. A.; Lester, H. A.; Dougherty, D. A., An intersubunit hydrogen bond in the nicotinic acetylcholine receptor that contributes to channel gating. *J. Biol. Chem.* **2008,** 283, (51), 35638-35643.
29. Moroni, M.; Zwart, R.; Sher, E.; Cassels, B. K.; Bermudez, I., Alpha4Beta2 nicotinic receptors with high and low acetylcholine sensitivity: pharmacology, stoichiometry, and sensitivity to long-term exposure to nicotine. *Mol. Pharmacol.* **2006,** 70, (2), 755-68.
30. Fonck, C.; Cohen, B. N.; Nashmi, R.; Whiteaker, P.; Wagenaar, D. A.; Rodrigues-Pinguet, N.; Deshpande, P.; McKinney, S.; Kwoh, S.; Munoz, J.; Labarca, C.;

Collins, A. C.; Marks, M. J.; Lester, H. A., Novel seizure phenotype and sleep disruptions in knock-in mice with hypersensitive alpha4 nicotinic receptors. *J. Neurosci.* **2005,** 25, (49), 11396-411.

31. Nowak, M. W.; Gallivan, J. P.; Silverman, S. K.; Labarca, C. G.; Dougherty, D. A.; Lester, H. A., *In vivo* incorporation of unnatural amino acids into ion channels in a *Xenopus* oocyte expression system. *Methods Enzymol.* **1998,** 293, 504-529.
32. Rodriguez, E. A.; Lester, H. A.; Dougherty, D. A., Improved amber and opal suppressor tRNAs for incorporation of unnatural amino acids *in vivo*. Part 1: Minimizing misacylation. *RNA* **2007,** 13, (10), 1703-1714.
33. Rodriguez, E. A.; Lester, H. A.; Dougherty, D. A., Improved amber and opal suppressor tRNAs for incorporation of unnatural amino acids *in vivo*. Part 2: Evaluating suppression efficiency. *RNA* **2007,** 13, (10), 1715-1722.
34. Dunsmore, C. J.; Carr, R.; Fleming, T.; Turner, N. J., A chemo-enzymatic route to enantiomerically pure cyclic tertiary amines. *J. Am. Chem. Soc.* **2006,** 128, (7), 2224-5.
35. Kash, T. L.; Jenkins, A.; Kelley, J. C.; Trudell, J. R.; Harrison, N. L., Coupling of agonist binding to channel gating in the $GABA_A$ receptor. *Nature* **2003,** 421, (6920), 272-5.
36. Price, K. L.; Millen, K. S.; Lummis, S. C., Transducing agonist binding to channel gating involves different interactions in 5-HT_3 and $GABA_C$ receptors. *J. Biol. Chem.* **2007,** 282, (35), 25623-30.
37. Venkatachalan, S. P.; Czajkowski, C., A conserved salt bridge critical for $GABA_A$ receptor function and loop C dynamics. *Proc. Natl. Acad. Sci. USA* **2008,** 105, (36), 13604-9.
38. Filatov, G. N.; White, M. M., The role of conserved leucines in the M2 domain of the acetylcholine receptor in channel gating. *Mol. Pharmacol.* **1995,** 48, (3), 379-84.
39. Labarca, C.; Nowak, M. W.; Zhang, H.; Tang, L.; Deshpande, P.; Lester, H. A., Channel gating governed symmetrically by conserved leucine residues in the M2 domain of nicotinic receptors. *Nature* **1995,** 376, 514-516.
40. Etter, J.-F., Cytisine for Smoking Cessation: A literature review and a meta-analysis. *Arch. Intern. Med.* **2006,** 166, (15), 1553-1559.
41. Mu, T. W.; Lester, H. A.; Dougherty, D. A., Different binding orientations for the same agonist at homologous receptors: A lock and key or a simple wedge? *J. Am. Chem. Soc.* **2003,** 125, (23), 6850-6851.
42. Puskar, N. L.; Xiu, X.; Lester, H. A.; Dougherty, D. A., Two neuronal nicotinic acetylcholine receptors, alpha4beta4 and alpha7, show differential agonist binding modes. *J. Biol. Chem.* **2011,** 286, (16), 14618-27.
43. Torrice, M. M., Chemical-scale studies of the nicotinic and muscarinic acetylcholine receptors. Ph.D. Thesis. California Institute of Technology, Pasadena, CA, **2009**.
44. Torrice, M. M.; Bower, K. S.; Lester, H. A.; Dougherty, D. A., Probing the role of the cation-π interaction in the binding sites of GPCRs using unnatural amino acids. *Proc. Natl. Acad. Sci. USA* **2009,** 106, (29), 11919-24.

45. Felpin; Girard, S.; Vo-Thanh, G.; Robins, R. J.; Villieras, J.; Lebreton, J., Efficient enantiomeric synthesis of pyrrolidine and piperidine alkaloids from tobacco. *J. Org. Chem.* **2001,** 66, (19), 6305-6312.